Hindawi Publishing Corporation
Journal of Chemistry
Volume 2013, Article ID 961629, 10 pages
http://dx.doi.org/10.1155/2013/961629

Research Article

Formation of Fe(0)-Nanoparticles via Reduction of Fe(II) Compounds by Amino Acids and Their Subsequent Oxidation to Iron Oxides

K. Klačanová,[1] P. Fodran,[2] P. Šimon,[3] P. Rapta,[3] R. Boča,[4] V. Jorík,[4] M. Miglierini,[5] E. Kolek,[6] and Ľ. Čaplovič[7]

[1] *Department of Nutrition and Food Assessment, Institute of Biochemistry, Nutrition and Health Protection, Faculty of Chemical and Food Technology, Slovak University of Technology, Radlinského 9, 812 37 Bratislava, Slovakia*
[2] *FLOP Inc., Mandľová 37, 851 10 Bratislava, Slovakia*
[3] *Department of Physical Chemistry, Institute of Physical Chemistry and Chemical Physics, Faculty of Chemical and Food Technology, Slovak University of Technology, Radlinského 9, 812 37 Bratislava, Slovakia*
[4] *Department of Inorganic Chemistry, Institute of Inorganic Chemistry, Technology and Materials, Faculty of Chemical and Food Technology, Slovak University of Technology, Radlinského 9, 812 37 Bratislava, Slovakia*
[5] *Department of Nuclear Physics and Technology, Institute of Nuclear and Physical Engineering, Faculty of Electrical Engineering and Information Technology, Slovak University of Technology, Ilkovičova 3, 812 19 Bratislava, Slovakia*
[6] *Food Research Institute, Priemyselná 4, P.O. Box 25, 824 75 Bratislava, Slovakia*
[7] *Institute of Materials Science, Faculty of Materials Science and Technology, Slovak University of Technology, Paulínska 16, 917 24 Trnava, Slovakia*

Correspondence should be addressed to K. Klačanová; katarina.klacanova@stuba.sk

Received 11 June 2012; Accepted 30 July 2012

Academic Editor: Gustavo Portalone

Iron nanoparticles were prepared by the reduction of central Fe(II) ion in the coordination compounds with amino acid ligands. The anion of the amino acid used as a ligand acted as the reducing agent. Conditions for the reduction were very mild; the temperature did not exceed 52°C, and the optimum pH was between 9.5 and 9.7. The metal iron precipitated as a mirror on the flask or as a colloid in water. Identification of the product was carried out by measuring UV/VIS spectra of the iron nanoparticles in water. The iron nanoparticles were oxidized by oxygen yielding a mixture of iron oxides. Oxidation of Fe(0) to Fe(II) took several seconds under air. The size and properties of iron oxide nanoparticles were studied by UV/VIS, TEM investigation, RTG diffractometry, Mössbauer spectroscopy, magnetometry, thermogravimetry, and GC/MS.

1. Introduction

The standard redox potential of the system Fe(II) → Fe(0) is −0.41 V and Fe(III) → Fe(0) is −0.04 V. Consequently, iron cannot be easily obtained by the reduction of its compounds [1]. Attention is paid to the preparation of micro- and nanoparticles of elementary iron. A well-known method for the preparation of iron microparticles is by thermal decomposition of iron pentacarbonyl, $Fe(CO)_5$, yielding particles of sizes within 500–700 nm [2]. The elementary iron prepared in this way is widely used in electronics (recording media, ferrites) and in pharmacy as an iron dietary supplement. It is also possible to prepare Fe(0) nanoparticles by the reduction of ferrous compounds with agents such as $NaBH_4$, N_2H_4, or NaH_2PO_2 in the presence of a protective colloid [3]; in that paper, the iron particles were reoxidized giving γ-Fe_2O_3 with a particle size of about 4 nm. An analogous method, without the protective colloid, led to Fe nanoparticles of the size 50–80 nm [4, 5]. Fe nanoparticles can also be prepared by the reduction of Fe(II) compounds by hydrogen at 700°C [6]. An efficient method for the preparation is the electrochemical reduction providing Fe nanoparticles with a diameter of

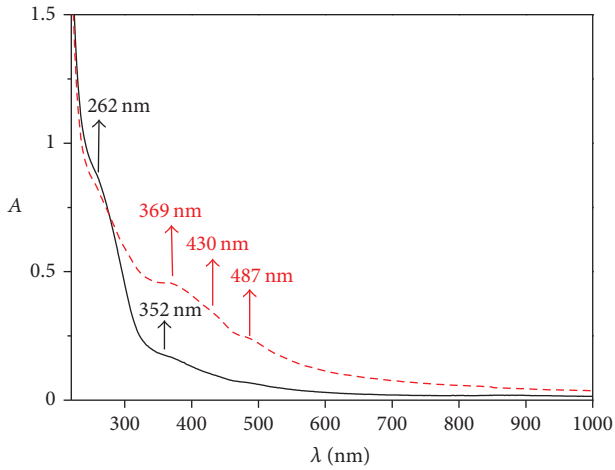

Figure 1: UV/VIS absorption spectra of Fe nanoparticles dispersed in water before (solid, black) and after opening to air (dashed, red).

nanoparticles about 39 nm [7, 8]. Biological reductions of Fe(II) to Fe(0) employing microorganisms have also attracted much attention [9–13]. Another interesting way of preparing Fe(0) nanoparticles is by the reduction of Fe(II) in transferrin by ascorbic acid [14]. Fe nanoparticles can also be prepared by the pyrolysis of organic Fe(II) salts, such as oxalates [15–17]. In this way it is possible to prepare a pyrophoric material applicable, inter alia, for military purposes [18].

In biological systems, reduction of Fe(II) to Fe(0) occurs very likely much easier. As an example, ferritins can be mentioned [19–21]. Samples of brain taken *post mortem* contain minerals, mainly goethite in protein nanotube. This mineral obviously cannot be physiologically active since it is insoluble, and it should not be encountered in living systems. Hence, it can be supposed that reduction of Fe(II) to Fe(0) takes place under anaerobic conditions. Subsequently, Fe(0) nanoparticles are spontaneously oxidized in the presence of oxygen so yielding iron oxides.

The aim of this paper is to prove that the formation of Fe nanoparticles by the reduction of Fe(II) to Fe(0) with amino acid ligands in the coordination sphere of the central Fe(II) atom in living systems is feasible.

2. Experimental

2.1. Materials. The amino acids, that is, phenylalanine (Phe), tryptophane (Trp), glycine (Gly), alanine (Ala), and glutamic acid (Glu) were purchased from Merck (Germany). Ferrous sulfate heptahydrate was obtained from Lachema (Czech Republic). Sodium hydroxide, diethylether, and anhydrous sodium sulfate were purchased from Microchem (Slovakia).

2.2. Apparatus. The products were analyzed by UV/VIS, transmission electron microscopy (TEM), RTG diffractometry, Mössbauer spectroscopy, magnetometry, TG/DTA, and GC/MS.

UV/VIS absorption spectra of iron nanoparticles were recorded employing a double-beam Shimadzu 3600 spectrometer. 1 mm quartz cuvette flow cell was used enabling the filling of the sample under an inert atmosphere.

The TEM investigations were performed on Philips CM 300 LaB_6 microscope. An accelerating voltage of 300 kV was used. A holey carbon film/copper net served as support of the nanoparticles.

X-ray (RTG) diffractometry was carried out using a Bragg-Brentano diffractometer Philips PW 1730/1050, using β-filtered CoK_α radiation, 40 kV/35 mA in the range of 3°–90° 2Θ, step 0.02°.

Mössbauer spectroscopy was performed in transmission geometry at room temperature (300 K). A conventional constant acceleration spectrometer working with a ^{57}Co/Rh source of radiation was employed. The experimentally measured spectra were fitted by the CONFIT evaluation software [22].

The magnetometry data were scanned by a SQUID magnetometer (MPMS-XL7, Quantum Design) in the DC detection mode. The measurements were conducted in two ways: (i) temperature dependence of the sample magnetic moment at temperatures from 1.9 to 300 K at constant magnetic field $B = 0.1$ T; (ii) field dependence of the sample magnetic moment within the range of B from 0 to 7 T at constant temperature $T = 4.6$ K.

Thermogravimetry (TG) measurements were performed using DTG-60 (Shimadzu). The temperature scale was calibrated to the fusion points of In, Sn, and Zn. The measurements were realized under oxygen and in an inert atmosphere of nitrogen at the heating rate of 10 K/min.

Gas chromatography (GC) was carried out using an Agilent Technologies 6890 gas chromatograph equipped with an Agilent Technologies 5973 inert mass selective spectrometer and with chromatographic column model no. J&W 122-503 E DB-5, 30 m × 0.25 mm × 0.5 μm.

2.3. Synthesis. A solution of 0.01 mol $Fe_2SO_4{\cdot}7H_2O$ in 300 mL of water (pH 7 ± 0.2) was placed in a three-necked flask with a magnetic stirrer, thermometer, tube for inert gas inlet and dropping funnel, and with external heating. The solution was purged with an inert gas (nitrogen or argon) and well stirred. When the solution in the flask was deaerated, the deareated solution of 0.02 mol of amino acid sodium salt in 50 mL of water was added in one portion. Within a few seconds, the complex of the amino acid with the Fe(II) cation was formed as a greyish-blue green dispersion. The dispersion in water was then very slowly heated. When the temperature reached 40°C, 0.04 mol of deareated solution of the sodium salt of the same amino acid in 100 mL water was added to the dispersion in one portion, and the pH was adjusted to 9.5–9.7 with the same amino acid. In the case of aliphatic amino acids, the reaction started immediately at this temperature. The reduction of aromatic amino acids needed a higher temperature, between 45 and 52°C. The metallic iron was quickly formed either as a metal mirror or as a yellow colloid. The colloid was transferred in an inert atmosphere from the flask to a cuvette for UV/VIS

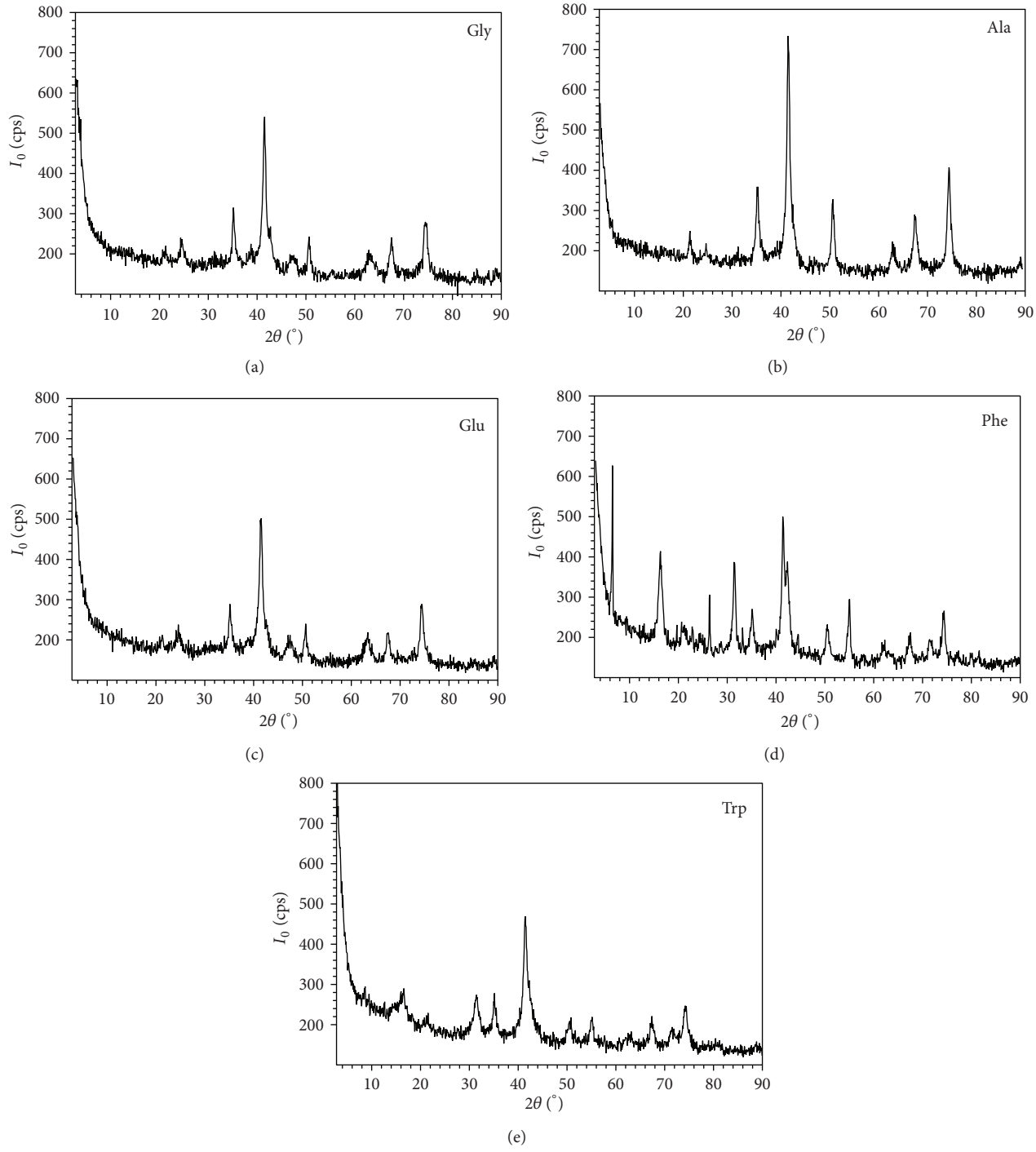

Figure 2: XRPD spectra of iron oxide nanoparticles. From top to bottom: samples Gly, Ala, Glu, Phe, Trp.

measurement. Then, the input of inert gas was stopped. The Fe(0) particles oxidized spontaneously with air or with oxygen to iron oxides. The oxides also form of a colloid in water. The UV/VIS spectra of the colloidal iron oxides were also recorded. Then, the orange-brownish precipitate was filtered using a Büchner funnel, well washed with demiwater and freely dried on air. The drying of the raw mixture of the iron oxides and organic by-products was purified by reflux, firstly with toluene and secondly with methylalcohol, again filtered with the Büchner funnel, washed with approx. 50 mL of diethylether and dried in air.

3. Results and Discussion

The reduction of Fe(II) coordination compounds by the anions of amino acids in an inert atmosphere is described here. In our paper [23], the amino acid degradation in the coordination sphere of Fe(II) complexes has been studied.

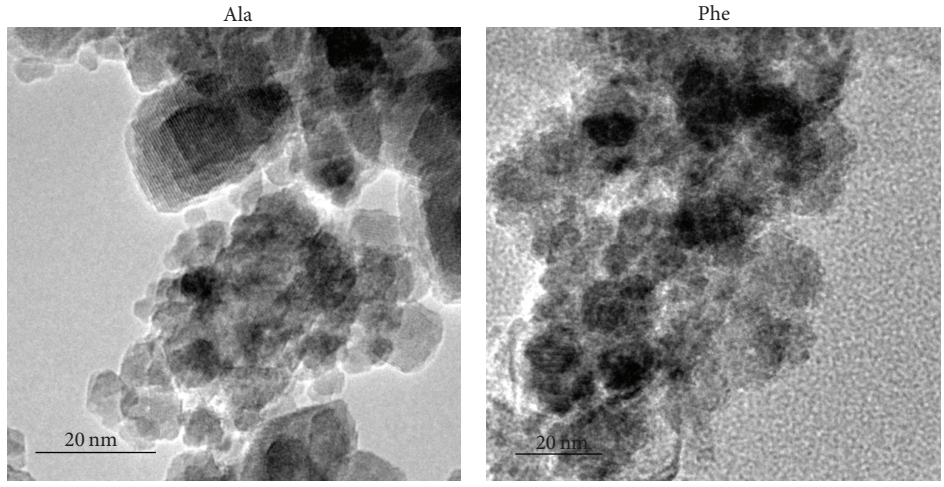

Figure 3: TEM photographies of iron oxide nanoparticles prepared by the reduction of Fe(II) with alanine and phenylalanine.

The degradation of amino acids took place between 20 and 25°C. Contrary to paper [23], a slight temperature increase leads to the reduction of the central Fe(II) atom to elemental iron instead of the expected degradation of amino acids since the reduction of Fe(II) to Fe(0) occurs between 40 and 52°C. Such a sharp temperature boundary is very atypical for the reduction of Fe(II). An exception is the reduction of ferrous cation to elemental iron by strong reducing agents, such as complex hydrides, hydrazine, or hypophosphites [4–6].

As mentioned previously, a small increase of temperature leads to reduction of the cation of the central atom to metal iron. In [23] we described a conceivable reaction mechanism of the amino acid degradation catalyzed with Fe(II) complexes where the products formed are carbonyl compounds or carboxylic acids. In the case of the reduction of the central Fe(II) atom, the amino acids yield different products. If phenylalanine was used as a reducing agent, the dominant products identified were amides of carboxylic acids, mainly phenylacetamide.

A spontaneous reduction of ferrous ions takes place in the range of pH 9.5–9.7. For pH higher than 9.7, a greater content of HO^- ions is present in the solution. The HO^- ion is a stronger electron-donor than the amino group so that it preferentially occupies the axial sites on the central Fe(II) ion where the reaction takes place [23]. A similar situation occurs if the amino acid in the form of a zwitterion is added to the water suspension of the complex; then, the carboxylate anion $O{=}C{-}O^-$ is the electron donor. At pH between 9.5 and 9.7, the $-NH_2$ group of the amino acid preferentially coordinates with the central Fe(II) ion [23]. The reactivity of the amino acid coordinated via the amino group obviously increases, so does the reactivity of the central Fe(II) ion. At lower temperature the degradation of amino acid takes place [23] while the reduction of the central ion to metallic iron occurs at increased temperature.

UV/VIS spectroscopy was employed to confirm the existence of the iron nanoparticles both in pristine and oxidized form. Figure 1 shows the UV-VIS absorption spectra of the Fe nanoparticles dispersed in water before and after opening to air. The optical spectra measured immediately after filling the sample under an inert atmosphere show a very similar pattern as found for pure Fe nanoparticles dispersed in water prepared by the electroexplosion of wires [24]. There is a broad peak at 352 nm and a peak at 262 nm. The peak at 352 nm is believed to be due to the remnants of collective oscillation of the surface plasmons. On keeping the sample under air, new absorption bands appeared due to oxidation with several maxima indicating various iron oxide nanoparticles.

Table 1: Size of iron-oxide nanoparticles determined by X-ray diffractometry [25, 26].

Abbr.	Origin	Crystallite size [nm]
(1) Gly	Glycine	10
(2) Ala	Alanine	10
(3) Glu	Glutamic acid	9
(4) Phe	Phenylalanine	8
(5) Trp	Tryptophane	11

Composition of the mixtures of iron oxides obtained by the oxidation of Fe(0)-nanoparticles, their size, and properties were studied by several methods. XRPD spectra of iron oxide nanoparticles are shown in Figure 2. The size of the iron oxide nanoparticles, calculated from the data of Figure 2 according to [25, 26], is listed in Table 1. As can be seen, the size of the nanoparticles is about 10 nm. This fact is also confirmed by TEM investigations (Figure 3).

Iron oxides present in nanoparticles were identified using Mössbauer spectroscopy. In addition to the degree of oxidation, structural states of iron ions were also determined. The Mössbauer spectra of the samples prepared with various amino acid anions as reducing agents are shown in Figure 4; the corresponding spectral parameters are listed in Table 2.

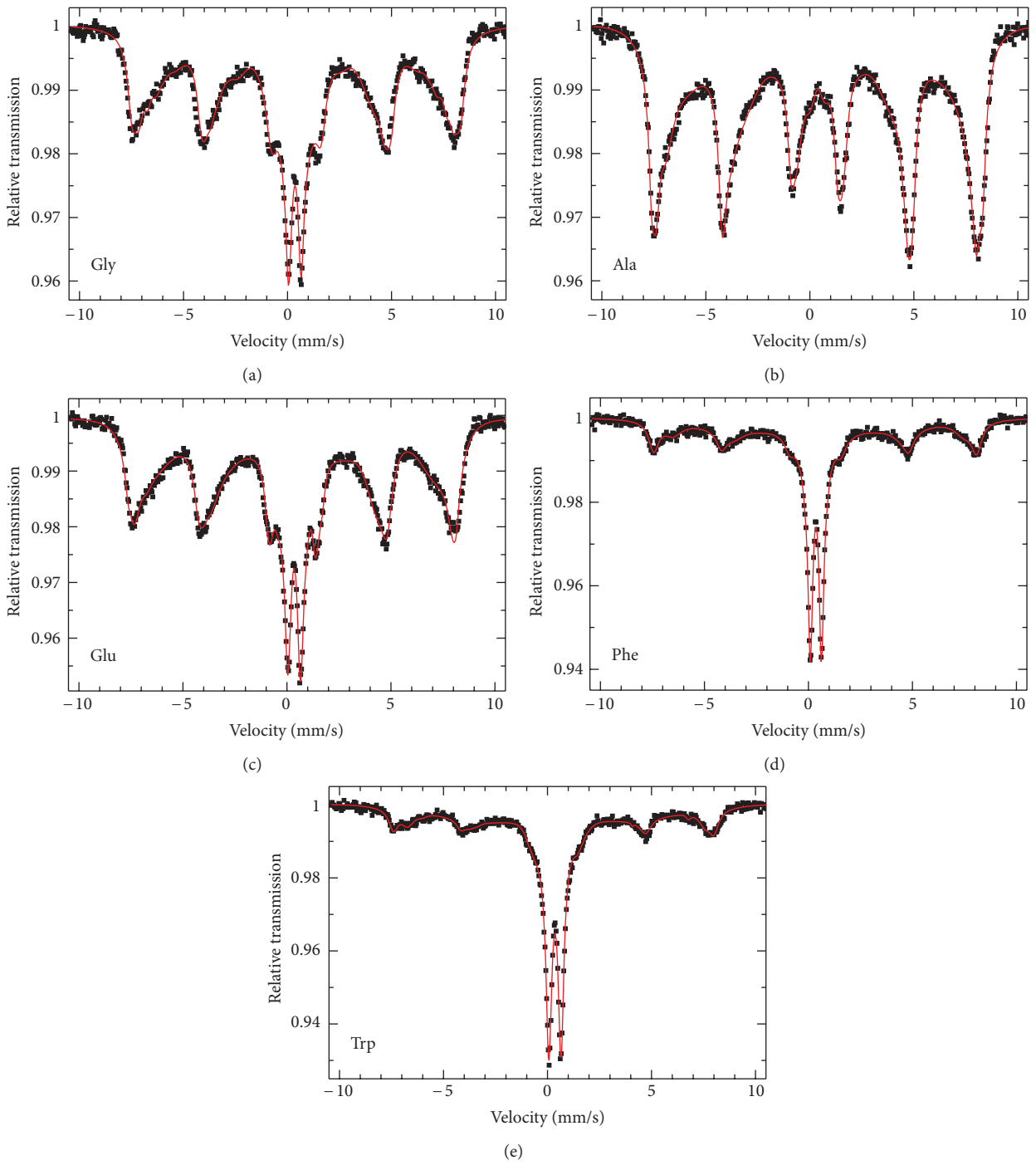

FIGURE 4: Room temperature ^{57}Fe Mössbauer spectra of the iron oxide nanoparticles. From top to bottom: samples 1—Gly, 2—Ala, 3—Glu, 4—Phe, 5—Trp.

It is noteworthy that a significant relative fraction of goethite (iron oxyhydroxide) was revealed in all measured samples.

The nanoparticles were further subjected to magnetic measurements. According to the recording functions (Figure 5), the samples can be divided into two groups. The first group includes the samples 1–3 with higher magnetoactivity which is manifested by the value of the mass susceptibility around $\chi_\rho = 400\,\mathrm{m^3\,kg^{-1}}$ and mass magnetization in saturation (at $B = 7\,\mathrm{T}$) over $M_\rho = 60\,\mathrm{A\,m^2\,kg^{-1}}$. Magnetization measurements were done in the mode of the field decreasing. The value of remnant magnetization was $M_r = 20\,\mathrm{A\,m^2\,kg^{-1}}$ (at $T = 4.6\,\mathrm{K}$) which is roughly one-third of the saturation value and can be deducted from the graphs. The samples show the magnetic hysteresis with the value of the coercive field $B_c = 0.03\,\mathrm{T}$. The second group includes the samples 4-5 with lower magnetoactivity which is manifested by the

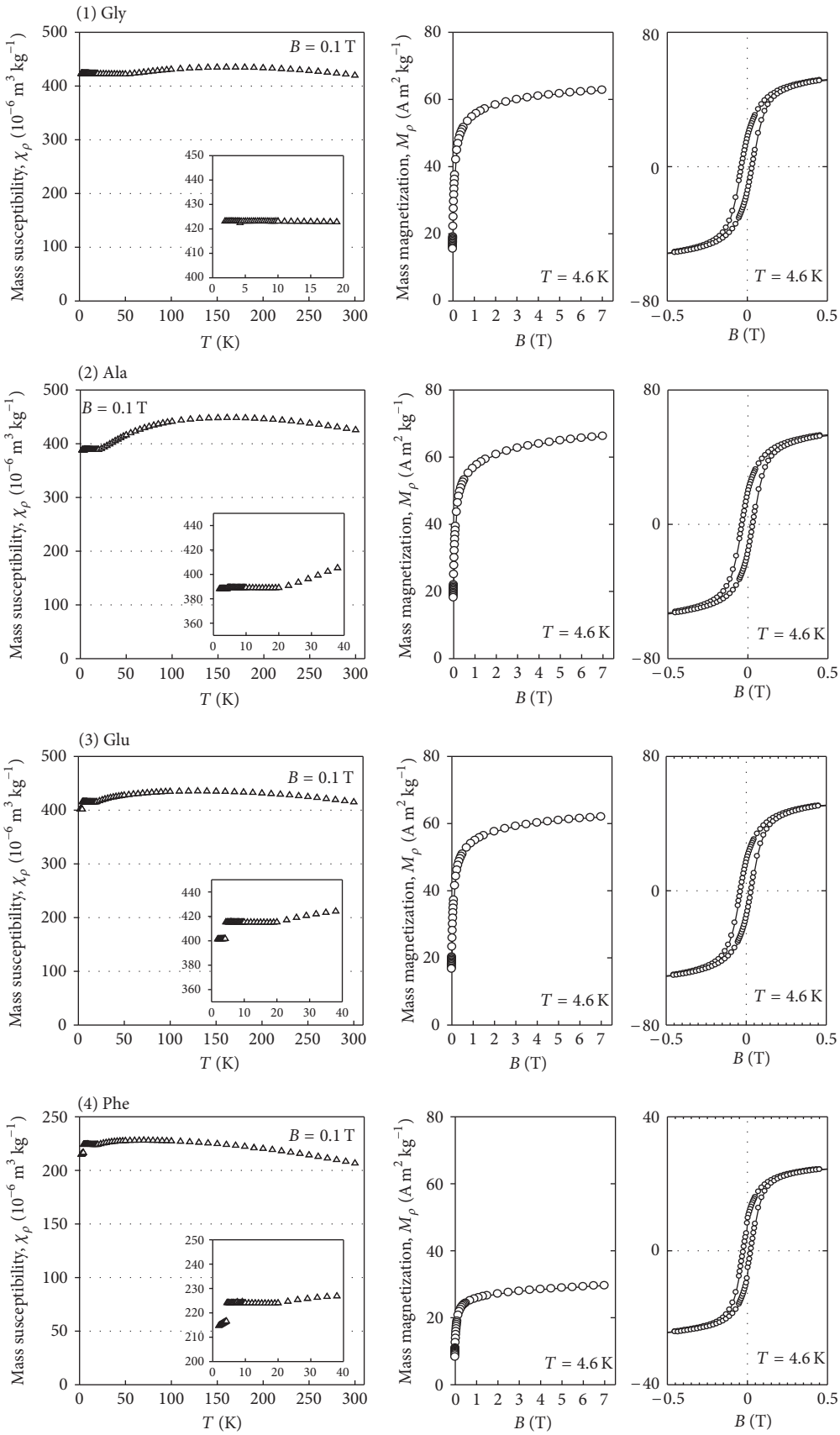

Figure 5: Continued.

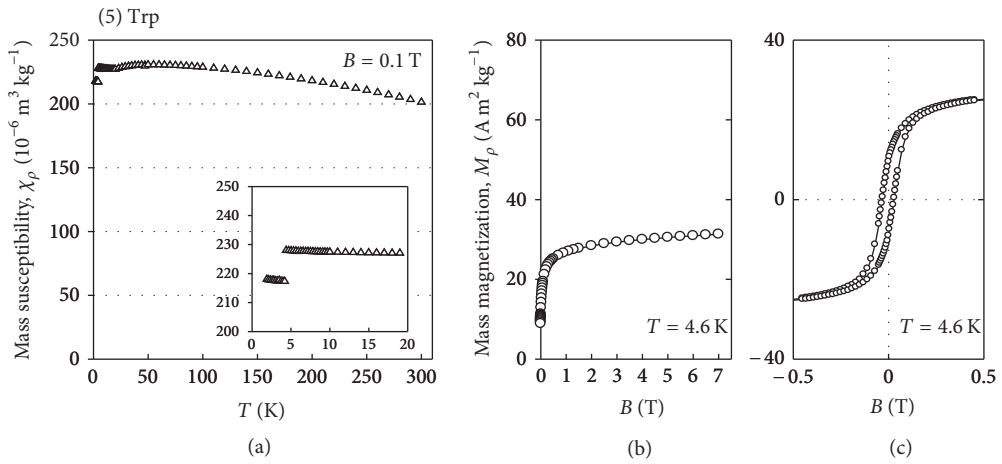

FIGURE 5: Magnetic functions for samples 1–5. (a) Temperature dependence of the mass magnetic susceptibility. (b) Field dependence of the mass magnetization. (c) Field dependence of magnetization demonstrating magnetic hysteresis. From top to bottom: samples 1—Gly, 2—Ala, 3—Glu, 4—Phe, 5—Trp.

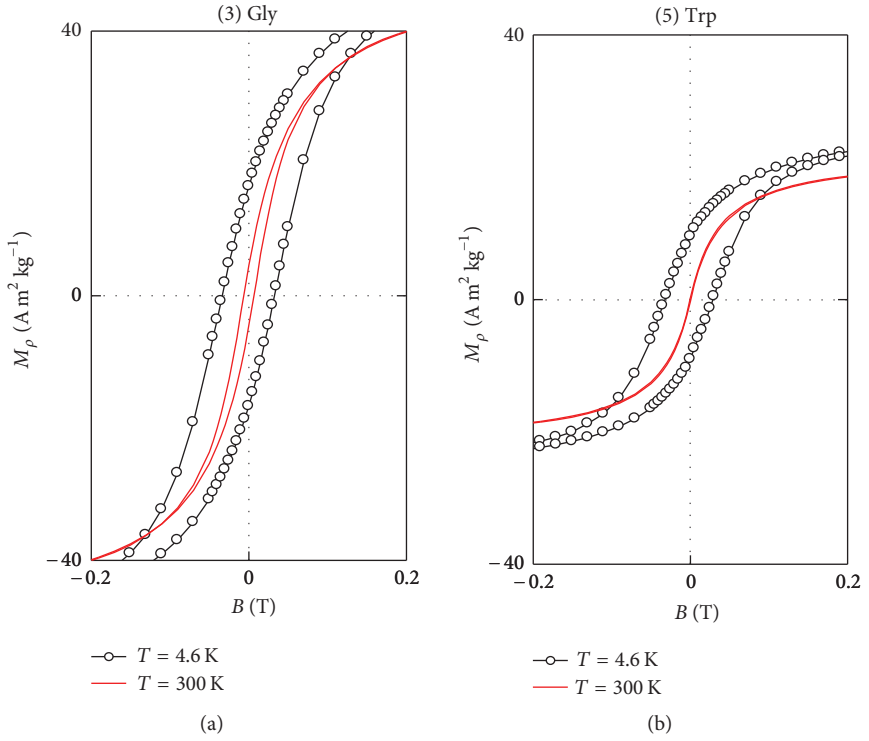

FIGURE 6: Magnetic hysteresis at helium and room temperature.

value of the mass susceptibility around $\chi_\rho = 200\,\text{m}^3\,\text{kg}^{-1}$ and mass magnetization at saturation (at $B = 7$ T) over $M_r = 30\,\text{A m}^2\,\text{kg}^{-1}$. These values are roughly half with regard to the first group. The value of remnant magnetization is $M_r = 10\,\text{A m}^2\,\text{kg}^{-1}$ (at $T = 4.6$ K), and it is one-third of the saturation value. The samples show the magnetic hysteresis with the value of the coercive field $B_c = 0.02$ T. On the basis of these facts, it can be summarized that the magnetoactivity of the second group of samples is about a half compared with the first group. The detection of magnetic hysteresis in both groups of samples at the experimental temperature is significant information. Increasing the temperature to room value, the profile of magnetic hysteresis is reduced (in the case of the complex 5, from the second group, hysteresis expires) (Figure 6).

The differences of magnetic moments depending on the amino acid anion are quite interesting. If the central Fe(II) ion is reduced by aliphatic amino acids, the magnetic moment of nanoparticles is higher than in the case of the reduction by aromatic amino acids. This difference can be brought

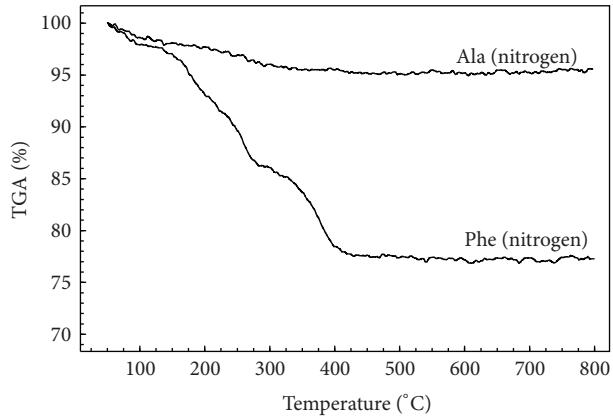

Figure 7: TG records of iron oxide nanoparticles prepared by the reduction of Fe(II) with alanine and phenylalanine, nitrogen atmosphere, heating rate 10 K/min.

Table 2: Spectral parameters derived from Mössbauer spectra of the investigated samples: A—spectral area, δ—isomer shift, B_{hf}—hyperfine field (only for sextets).

Sample	Component	δ (mm s^{-1})	B_{hf} (T)	A (%)
(1) Gly	α-Fe_3O_4 (magnetite)	0.42	49.0	12
	β-Fe_3O_4 (magnetite)	0.45	44.6	6
	γ-Fe_2O_3 (maghemite)	0.42	47.0	18
	α-FeOOH (goethite)	0.52	33.9	41
	high spin Fe^{3+}	0.35	0.60*	11
	low spin Fe(III)	0.42	1.10*	12
(2) Ala	α-Fe_3O_4 (magnetite)	0.35	49.4	12
	β-Fe_3O_4 (magnetite)	0.45	45.8	19
	γ-Fe_2O_3 (maghemite)	0.32	47.8	15
	α-FeOOH (goethite)	0.39	32.6	53
	high spin Fe^{3+}	0.35	0.60*	1
(3) Glu	α-Fe_3O_4 (magnetite)	0.26	49.0	4
	β-Fe_3O_4 (magnetite)	0.67	46.0	3
	γ-Fe_2O_3 (maghemite)	0.32	47.7	21
	α-FeOOH (goethite)	0.36	33.5	55
	high spin Fe^{3+}	0.34	0.60*	17
(4) Phe	γ-Fe_2O_3 (maghemite)	0.32	48.2	18
	α-FeOOH (goethite)	0.35	33.3	44
	high spin Fe^{3+}	0.36	0.53*	29
	low spin Fe(III)	0.36	0.97*	9
(5) Trp	γ-Fe_2O_3 (maghemite)	0.30	47.6	9
	α-FeOOH (goethite)	0.40	32.3	56
	high spin Fe^{3+}	0.36	0.58*	35
	γ-Fe_2O_3 (maghemite)	0.32	47.8	10
	α-FeOOH (goethite)	0.27	29.7	32

*Quadrupole splitting E_Q (mm s^{-1}).

about by occlusion of degradation products of amino acids in agglomerates of iron oxide nanoparticles; the agglomerates are formed readily due to the magnetic properties of the nanoparticles. Preliminary thermogravimetry measurements revealed that the content of organic matter in the iron oxide nanoparticles was quite high. Therefore, the nanoparticles were purified by extraction with toluene and methanol. The aliphatic amino acids used for the reduction of Fe(II) oxidize yielding low-molecular liquid products which can be extracted by the organic solvents. The aromatic amino acids oxidize giving crystalline products with high temperatures of decomposition; these compounds cannot be extracted fully by the solvents used. This can be clearly seen comparing the TG records of iron oxide nanoparticles (Figure 7) where sodium alaninate and sodium phenylalaninate were used as the reducing agents. In the case of sodium alaninate, the mass loss of nanoparticles is about 3% up to 450°C; this mass loss corresponds obviously to the loss of occluded solvents (up to 150°C) and the loss of water by dehydroxylation at higher temperatures. In case of sodium phenylalaninate, the mass loss occurs in two stages where the total mass loss is 21% up to 450°C. The first stage corresponds to the decomposition of benzamide, the other one to the decomposition of phenylacetamide. Both compounds were identified by GC/MS. TG studies thus confirm that aliphatic amino acids provide purer nanoparticles.

A presumptive mechanism of the reduction is shown in Scheme 1. At low temperature, only one ligand binds to the axial site of the complex as an anion of the amino acid [23]. Contrary to the destruction of amino acids by Fe(II) complexes, at higher temperatures two anions of the amino acid are bound to the two axial sites. Such a complex compound may be unstable, and a concerted redox reaction takes place both at the central cation Fe(II) and the ligands bound at the axial sites. As seen from Scheme 1, the amino acid is oxidized at the α-carbon atom simultaneously splitting off formiate anion. Thus, an amide of the acid, shorter by one carbon atom than the original amino acid, is formed. Since the reaction occurs simultaneously at both anions of the amino acid bound at the axial sites, two formiate anions may reduce Fe(II) to Fe(0) by the single-electron transfer under the liberation of CO_2. The protons formed are neutralized with OH^- anions which leads to a slight decrease of pH which was observed. The proposed mechanism elucidates the formation of Fe nanoparticles as well as of amides of carboxylic acids.

We also tried to reduce other transition metal cations as central atoms in coordination compounds with the ligands mentioned here. Co(II), Cu(II) and Mn(II) are not reduced under the conditions described. Exclusively, the reduction of Fe(II) complexes to Fe(0) with amino acids takes place upon the formation of nanoparticles.

4. Conclusions

A method for the formation of iron and iron oxide nanoparticles by the reduction of the central Fe(II) ion in the coordination compounds with amino acid ligands is described. The anion of the amino acid used as a ligand acts as the reducing agent. Conditions for the reduction are very mild; the temperature does not exceed 52°C, and the optimum pH is between 9.5 and 9.7. The process is very rapid; under the

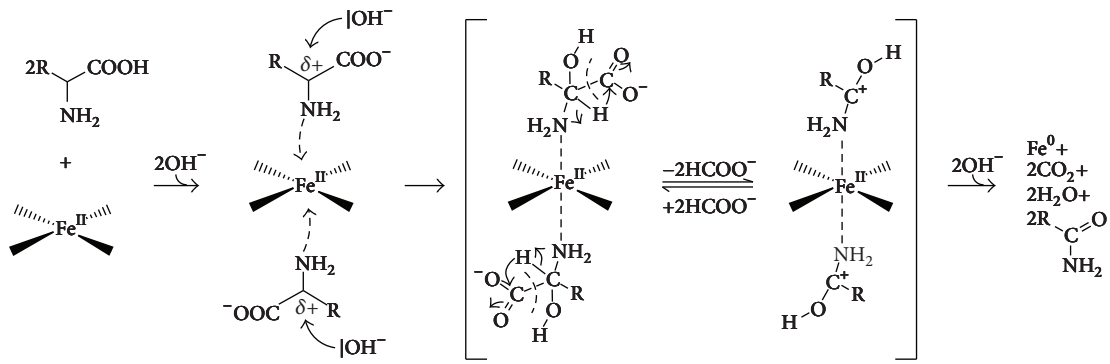

Scheme 1: Suggested mechanism of the reduction of Fe(II) to Fe(0) with amino acid ligands in the coordination sphere of central Fe(II) atom.

conditions mentioned, the reduction is finished within a few seconds. A mechanism of the reduction is suggested.

The metal iron precipitates as a mirror on the flask or as a colloid in water. It is impossible to isolate the metal iron prepared in this way due to the very small size of the particles. For this reason the identification of the product was carried out by measuring UV/VIS spectra of the iron nanoparticles in water. The iron nanoparticles were oxidized by oxygen yielding a mixture of iron oxides. Oxidation of Fe(0) to Fe(II) is also very rapid; it takes several seconds under air. The size and properties of iron oxides were studied by UV/VIS, TEM investigation, RTG diffractometry, Mössbauer spectroscopy, magnetometry, thermogravimetry, and GC/MS.

Reduction of Fe(II) by aliphatic amino acid anions runs slightly above the physiological temperature so that a similar reduction in nonheme types of metalloenzymes is likely. This could account for the course of some feverish diseases or could lead to *in situ* synthesis of iron oxide nanoparticles for diagnostic and treatment.

Acknowledgment

Financial support from Slovak grant agencies (VEGA 1/0052/11, 1/0220/12, 1/0233/12, 1/0882/13 and APVV-0014-11, APVV-VVCE 0004-07) is gratefully acknowledged. M. Miglierini also acknowledges the support by the Operational Program Research and Development for Innovations, European Regional Development Fund (Project CZ.1.05/2.1.00/03.0058) and Operational Program Education for Competitiveness, European Social Fund (Project CZ.1.07/2.3.00/20.0017).

References

[1] M. Radivojević, T. Rehren, E. Pernicka, D. Šljivar, M. Brauns, and D. Borić, "On the origins of extractive metallurgy: new evidence from Europe," *Journal of Archaeological Science*, vol. 37, no. 11, pp. 2775–2787, 2010.

[2] S. Jia, F. Luo, Y. Qing, W. Zhou, and D. Zhu, "Electroless plating preparation and microwave electromagnetic properties of Ni-coated carbonyl iron particle/epoxy coatings," *Physica B*, vol. 405, no. 17, pp. 3611–3615, 2010.

[3] H. Iida, T. Nakanishi, H. Takada, and T. Osaka, "Preparation of magnetic iron-oxide nanoparticles by successive reduction-oxidation in reverse micelles: effects of reducing agent and atmosphere," *Electrochimica Acta*, vol. 52, no. 1, pp. 292–296, 2006.

[4] G. C. C. Yang and H. L. Lee, "Chemical reduction of nitrate by nanosized iron: kinetics and pathways," *Water Research*, vol. 39, no. 5, pp. 884–894, 2005.

[5] N. Xiaomin, S. Xiaobo, Z. Huagui, Z. Dongen, Y. Dandan, and Z. Qingbiao, "Studies on the one-step preparation of iron nanoparticles in solution," *Journal of Crystal Growth*, vol. 275, no. 3-4, pp. 548–553, 2005.

[6] J. M. Pang, P. M. Guo, P. Yhao, C. Z. Cao, D. G. Zhao, and D. G. Wang, "Reduction of 1–3 mm iron ore by H_2 in a fluidized bed," *International Journal of Minerals, Metallurgy, and Materials*, vol. 16, pp. 620–625, 2009.

[7] M. Z. Kassaee, E. Motamedi, A. Mikhak, and R. Rahnemaie, "Nitrate removal from water using iron nanoparticles produced by arc discharge vs. reduction," *Chemical Engineering Journal*, vol. 166, no. 2, pp. 490–495, 2011.

[8] Y. X. Chen, S. P. Chen, Q. S. Chen, Z. Y. Zhou, and S. G. Sun, "Electrochemical preparation of iron cuboid nanoparticles and their catalytic properties for nitrite reduction," *Electrochimica Acta*, vol. 53, no. 23, pp. 6938–6943, 2008.

[9] T. X. Liu, X. M. Li, F. B. Li, W. Zhang, M. J. Chen, and S. G. Zhou, "Reduction of ironoxides by *Klebsiella pneumoniae* L17: kinetics and surfaceproperties," *Colloids and Surfaces A*, vol. 379, no. 1–3, pp. 143–150, 2011.

[10] R. E. Cowart, "Reduction of iron by extracellular iron reductases: implications for microbial iron acquisition," *Archives of Biochemistry and Biophysics*, vol. 400, no. 2, pp. 273–281, 2002.

[11] E. C. Salas, W. M. Berelson, D. E. Hammond, A. R. Kampf, and K. H. Nealson, "The impact of bacterial strain on the products of dissimilatory iron reduction," *Geochimica et Cosmochimica Acta*, vol. 74, no. 2, pp. 574–583, 2010.

[12] J. W. Stucki and J. E. Kostka, "Microbial reduction of iron in smectite," *Comptes Rendus*, vol. 338, no. 6-7, pp. 468–475, 2006.

[13] I. Schröder, E. Johnson, and S. de Vries, "Microbial ferric iron reductases," *FEMS Microbiology Reviews*, vol. 27, no. 2-3, pp. 427–447, 2003.

[14] J. M. May, Z. C. Qu, and S. Mendiratta, "Role of ascorbic acid in transferrin-independent reduction and uptake of iron by U-937 cells," *Biochemical Pharmacology*, vol. 57, no. 11, pp. 1275–1282, 1999.

[15] A. Schmid, US Pat 2 096 009, October 1937.

[16] P. Pranda, V. Hlavacek, and M. L. Markowski, "Ultrafine iron powder as an oxygen scavenger for argon purification. Active iron from organic precursors," *Industrial and Engineering Chemistry Research*, vol. 41, no. 19, pp. 4837–4840, 2002.

[17] R. Shende, A. Vats, Z. Doorenbos, D. Kapoor, and J. Puszynski, "Formation of pyrophoric alpha-Fe nanoparticles from Fe(II)-oxalate," in *Proceedings of the NSTI Nanotechnology Conference and Trade Show (NSTI Nanotech '08)*, M. Laudon and B. Romanowicz, Eds., p. 692, CRC Press, Boston, Mass, USA, June 2008.

[18] R. Shende, Z. Doorenbos, A. Vats, J. Puszynski, D. Kapoor, and D. Martin, "Pyrophoric nanoparticles and nanoporous foils for defense applications," in *Proceedings of the 26th Army Science Conference*, Orlando, Florida, 2008.

[19] E. C. Theil, "Ferritin protein nanocages use ion channels, catalytic sites, and nucleation channels to manage iron/oxygen chemistry," *Current Opinion in Chemical Biology*, vol. 15, no. 2, pp. 304–311, 2011.

[20] C. Quintana, J. M. Cowley, and C. Marhic, "Electron nanodiffraction and high-resolution electron microscopy studies of the structure and composition of physiological and pathological ferritin," *Journal of Structural Biology*, vol. 147, no. 2, pp. 166–178, 2004.

[21] A. V. Alekseenko, T. V. Waseem, and S. V. Fedorovich, "Ferritin, a protein containing iron nanoparticles, induces reactive oxygen species formation and inhibits glutamate uptake in rat brain synaptosomes," *Brain Research*, vol. 1241, pp. 193–200, 2008.

[22] T. Žák and Y. Jirásková, "CONFIT: Mössbauer spectra fitting program," *Surface and Interface Analysis*, vol. 38, no. 4, pp. 710–714, 2006.

[23] K. Klačanová, P. Fodran, and M. Rosenberg, "The possible production of natural flavours by amino acid degradation," *Monatshefte fur Chemie*, vol. 141, no. 7, pp. 823–828, 2010.

[24] O. P. Siwach and P. Sen, "Fluorescence properties of Fe nanoparticles prepared by electro-explosion of wires," *Materials Science and Engineering B*, vol. 149, no. 1, pp. 99–104, 2008.

[25] A. C. Larson and R. B. von Dreele, "General Structure Analysis System (GSAS)," Report LAUR 86-748, Los Alamos National Laboratory, Los Alamos, NM, USA, 2004.

[26] B. H. Toby, "EXPGUI: a graphical user interface for GSAS," *Journal of Applied Crystallography*, vol. 34, pp. 210–213, 2001.